BMC Medical Genomics

RESEARCH

Open Access

A machine learning model and identification of immune infiltration for chronic obstructive pulmonary disease based on disulfidptosis-related genes

Sijun Li[1†], Qingdong Zhu[2†], Aichun Huang[2], Yanqun Lan[2], Xiaoying Wei[2], Huawei He[2], Xiayan Meng[2], Weiwen Li[2], Yanrong Lin[2*] and Shixiong Yang[3*]

Abstract

Background Chronic obstructive pulmonary disease (COPD) is a chronic and progressive lung disease. Disulfidptosis-related genes (DRGs) may be involved in the pathogenesis of COPD. From the perspective of predictive, preventive, and personalized medicine (PPPM), clarifying the role of disulfidptosis in the development of COPD could provide a opportunity for primary prediction, targeted prevention, and personalized treatment of the disease.

Methods We analyzed the expression profiles of DRGs and immune cell infiltration in COPD patients by using the GSE38974 dataset. According to the DRGs, molecular clusters and related immune cell infiltration levels were explored in individuals with COPD. Next, co-expression modules and cluster-specific differentially expressed genes were identified by the Weighted Gene Co-expression Network Analysis (WGCNA). Comparing the performance of the random forest (RF), support vector machine (SVM), generalized linear model (GLM), and eXtreme Gradient Boosting (XGB), we constructed the ptimal machine learning model.

Results DE-DRGs, differential immune cells and two clusters were identified. Notable difference in DRGs, immune cell populations, biological processes, and pathway behaviors were noted among the two clusters. Besides, significant differences in DRGs, immune cells, biological functions, and pathway activities were observed between the two clusters.A nomogram was created to aid in the practical application of clinical procedures. The SVM model achieved the best results in differentiating COPD patients across various clusters. Following that, we identified the top five genes as predictor genes via SVM model. These five genes related to the model were strongly linked to traits of the individuals with COPD.

†Sijun Li and Qingdong Zhu contributed equally to this work.

*Correspondence:
Yanrong Lin
linyanrong2009@126.com
Shixiong Yang
13407719256@163.com

Full list of author information is available at the end of the article

Conclusion Our study demonstrated the relationship between disulfidptosis and COPD and established an optimal machine-learning model to evaluate the subtypes and traits of COPD. DRGs serve as a target for future predictive diagnostics, targeted prevention, and individualized therapy in COPD, facilitating the transition from reactive medical services to PPPM in the management of the disease.

Keywords Chronic obstructive pulmonary disease, Disulfidptosis, Disulfidptosis-related genes, Immune cells, Machine learning model

Introduction

As is well documented, chronic obstructive pulmonary disease (COPD) is a chronic and progressive lung disease characterized by respiratory symptoms associated with chronic airflow restriction, and clinical features include chronic bronchitis, small airway destruction, and alveolar enlargement/disturbance [1, 2]. According to a 2018 study, approximately 300 million people suffer from COPD worldwide, causing about 3.2 million death each year [3]. The diagnosis rate of COPD patients ranges from 23.61 to 30.00% in China [4]. With global aging and an elevated smoking population, the incidence of COPD is also on the rise, which not only puts a burden on healthcare systems but also leads to a heavy financial burden [5–10]. To better manage COPD, Zhu et al. suggested that COPD individuals may gain more benefit through predictive, preventive, and personalized medicine (PPPM) than current "one-sizefits-all" approach [11].

Regrettably, a large proportion of COPD patients suffer from missed diagnoses or misdiagnoses [12, 13]. The diagnosis of COPD largely relies on pulmonary function tests to determine the degree of airflow restriction (i.e., forced expiratory volume (FEV1)/ forced vital capacity (FVC) < 0.7 after bronchodilator use for COPD diagnosis) [14]. However, the spirometry may not be readily available. Therefore, it is imperative to discover more accurate methods to assist clinicians in diagnosing COPD. Previous studies designed predictive models based on specific molecular markers for the diagnosis of diseases [15–17], which can strongly encourage the transition from reactive to PPPM [18].

To establish a predictive model of COPD, its pathogenesis must first be elucidated. Immunoinflammation [19], cell senescence [20], and proteolysis [21] are postulated to participate in the pathogenesis of COPD, ultimately leading to the death of lung cells [22–25]. Liu et al. demonstrated that cell death-related mechanism could serve as a promising tool for PPPM. Disulfidptosis, a novel cell death mechanism, is caused by disulfide stress induced by aberrant accumulation of cystine (Gys, a disulfide with high cytotoxicity) [26–28]. Under physiological conditions, glucose generates a reduced form of nicotinamide adenine dinucleotide phosphate (NADPH) via the pentose phosphate pathway, thereby providing a key reducing capacity to counteract the toxic effects of disulfide stress on cells. However, excessive cystine uptake and cystine reduction to cysteine (Gyss) deplete the NADPH pool under hypoglycemic states, while actin increases the cell's sensitivity to disulfide stress, eventually promoting massive accumulation of disulfide molecules and rapid cell death [29, 30]. In this process, the members of the solute carrier family, namely SLC7A11 and SLC3A2, form complexes that trigger the entry of extracellular cystine into cells, which can also cause abnormal disulfide bonding in the cytoskeleton protein actin and F-actin collapse [25]. Beeh et al. found increased disulfide concentration in the sputum of COPD patients [31], signaling that disulfidptosis may be implicated in the pathogenesis of COPD. Therefore, a comprehensive understanding of disulfidptosis-related genes (DGRs) might provide insights for the PPPM strategy for COPD.

However, the role of the DRGs in the pathogenesis of COPD remains elusive. The purpose of the current study was to establish a diagnostic model based on differentially expressed disulfidptosis-related genes (DE-DRGs) to improve the accuracy and convenience of COPD diagnosis and provide additional candidate biomarkers for clinical research, as well as the diagnosis and treatment of COPD.

Materials and methods

Experimental design

The experimental design is illustrated in Fig. 1.

Data acquisition and pre-processing

Two datasets (GSE38974 and GSE76925), both including healthy individuals and COPD individuals, were retrieved from the GEO database (https://www.ncbi.nlm.nih.gov/gds). As stated above, the two data matrices included healthy individuals and COPD patients. They were preprocessed by Perl language according to our previous method [32]. The GSE38974 dataset (GPL4133 platform), including lung tissue samples from 9 healthy individuals (control group) and 23 COPD individuals (COPD group), were selected for further analysis [33]. Meanwhile, the GSE76925 dataset (GPL10558 platform), including lung tissue samples from 40 healthy individuals and 111 COPD individuals, was selected for validation [34]. The following clinical characteristics were extracted from the GSE76925 dataset: body mass index (BMI), forced expiratory volume in 1 s, percent predicted (FEV1.PP), ratio

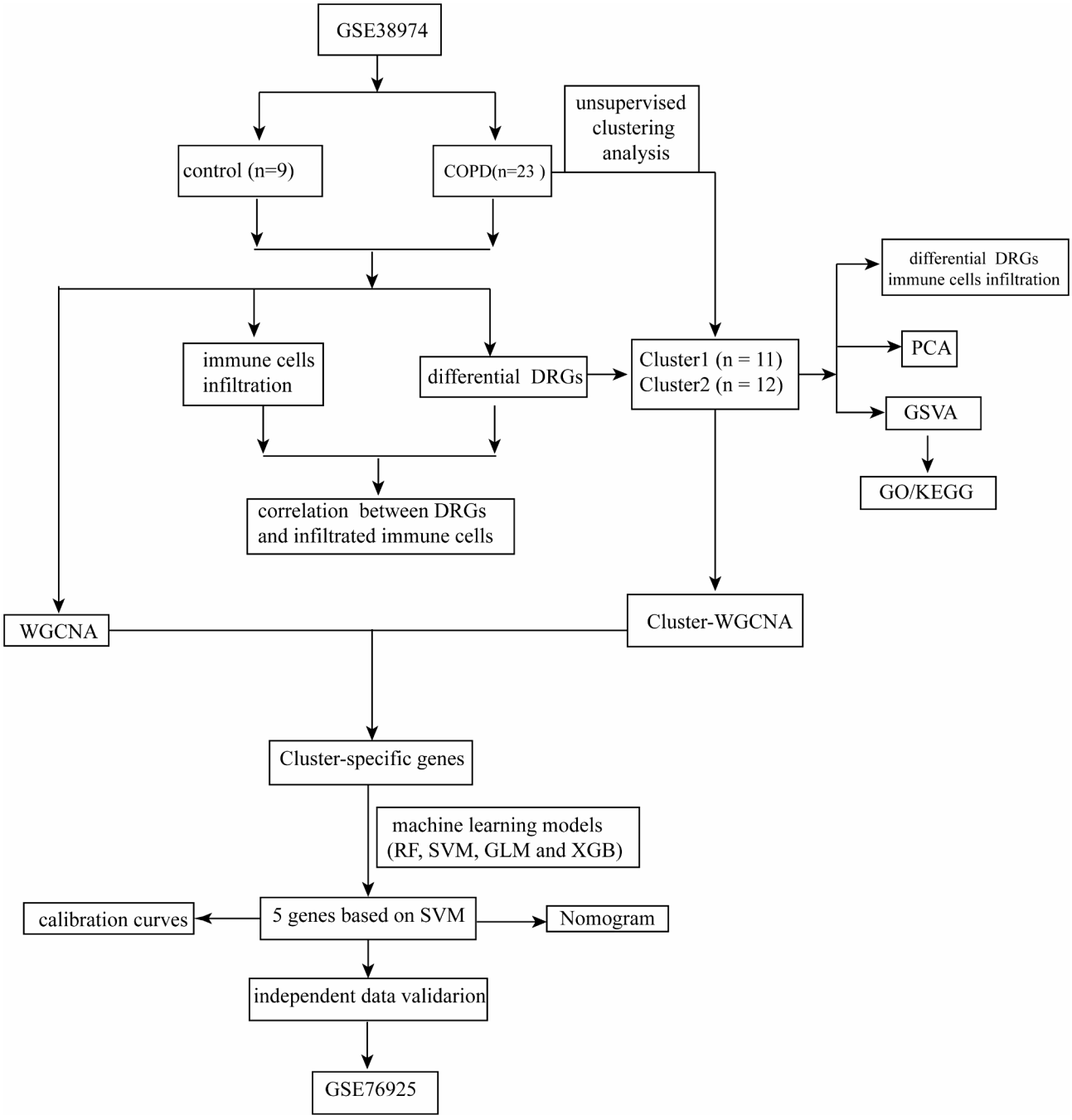

Fig. 1 Experimental design was exhibited

of FEV1 to forced vital capacity (FEV1/FVC), low attenuation areas at − 950 HU on chest computed tomography (CT) scans (LAA950), 15th percentile of the lung density histogram on chest CT scans (perc15), and square root wall area of a hypothetical airway with 10 mm internal perimeter (Pi10) [34]. DRGs were obtained from the study of Deal et al. [35]. The R Programming Language(version 4.1.3) was utilized in this study.

Identification of DE-DGRs in COPD

The "limma" R package was employed to screen DE-DRGs from the GSE38974 dataset. The "ggpubr" R package and "pheatmap" R package was used to construct the box plot and heatmap, respectively. The "corrplot" R package was applied to correlate DE-DRGs and explore their correlations.

Assessing the immune cell infiltration

COPD is a state of prolonged chronic inflammation [18]. Therefore, the difference in immune cell infiltration between the normal control group and the COPD group was examined. CIBERSORTx is a general-purpose gene expression-based deconvolution algorithm that quantifies cellular components from the gene expression profile of a tissue [36]. The methods used to assess the infiltration of immune cells refer to our previous study [32]. Single-sample gene-set enrichment analysis (ssGSEA) was employed to generate abundance score of. immune cell infiltration [37]. Samples with $p < 0.05$ were selected to generate the immune cell infiltration matrix via ssGSEA.

Correlation analysis between DGRs and infiltrated immune cells

In order to further illustrate the connection between DGRs and the attributes of pertinent immune cells, the correlation coefficient was calculated to determine the relationship between DE-DRG expression and the proportion of immune cells. A correlation was considered significant if the p-value, as determined by the Spearman correlation coefficient, was less than 0.05. Ultimately, the outcomes were displayed utilizing the R package called 'corrplot'.

Clustering of COPD patients

Using the expression profile of DGRs, we utilized the 'ConsensusClusterPlus' R package to conduct unsupervised clustering analysis on a group of 23 COPD patients, classifying them into distinct subtypes.By setting the k value from 1 to 9, various subtypes were created, and the ideal cluster count was chosen based on the consensus score. Principal component analysis (PCA)was utilized to visualize the distribution of the two subtypes.

Gene set variation analysis (GSVA)

The "GSVA" R package was utilized for conducting GSVA enrichment analysis and assessing variations in enriched gene sets among the various DGR clusters.The symbols 'c5.go.symbols' and 'c2.cp.kegg.symbols' were obtained from the MSigDB database.To identify differential expression pathways and biological functions, the limma R package (version 4.13) was utilized to compare GSVA scores among the various clusters of DGRs.A P-value less than 0.05 is regarded as a statistically significant distinction.

The "GSVA" R package was employed for GSVA enrichment analysis and to evaluate differences in enriched gene sets among the different DGR clusters. The "c5.go.symbols" and "c2.cp.kegg.symbols:" were acquired from the MSigDB database. The "limma" R package (version 4.13) was applied to identify differential expression pathways and biological functions by comparing GSVA scores between the different DGRs clusters. A P-value < 0.05 is considered a statistically significant difference.

Weighted gene co-expression network analysis (WGCNA)

The "WGCNA" R package was utilized to establish the WGCNA co-expression module.Following our previous studies, we constructed disease WGCNA and clusters WGCNA [32]. We selected the genes in the module with the greatest significance and the smallest p-value from disease WGCNA and clusters WGCNA, and intersected the genes in the two modules. The intersection-genes are used to build machine learning models [32].

Construction and validation of a nomogram model

To investigate COPD clusters, nomogram models were constructed using the "rms" R package. Nomogram models were by using the 'rms' R package to assess COPD clusters. A score was given to each predictor, and the sum of all predictor scores resulted in the 'total score'. To assess the predictive ability of the nomogram model, the calibration curve and DCA were employed.

Construction of predictive model based on multiple machine learning methods

The 23 COPD samples from GSE38974 dataset were classified as a training set. The 109 COPD samples from GSE76925 dataset were classified as a testing set. The input dimension in GSE38974 dataset was as follows: 32, 19695; The input dimension in GSE76925 dataset was as follows:151, 25222. To construct machine learning models which includes the random forest (RF) model, support vector machine (SVM) model, generalized linear model (GLM), and eXtreme Gradient Boosting (XGB), we utilized the 'caret' R package. The hyperparameters of each machine learning model were as follows: RF: ntree: 500, mtry: 3, nodesize: 1; SVM: C: 1, sigma: caret, prob.model: true; GLM: family: binomial; XGB: nrounds: 150, maxdepth: 6, eta: 0.3, gamma: 0,subsample: 1, colsample_bytree: 1, lambda: 1. The "pROC" R pages visualized the area below the ROC curve.The key predictive genes associated with COPD were regarded as the top 5 significant variables in the optimal machine learning model.To examine the diagnostic significance of the model, an analysis of the receiver operating characteristic (ROC) curve was conducted using the GSE76925 dataset. Subsequently, a correlation analysis was performed on the clinical characteristics of 109 COPD patients in the GSE76925 dataset, using the identified key predictive genes for COPD.

Results

Identification of DE-DRGs in COPD

To clarify the role of DRGs in the advancement and growth of COPD, we utilized the GSE38974 dataset to assess their expression profile in both the control and COPD groups.We revealed the four genes as DE-DRGs (Fig. 2a). In COPD, the levels of NDUFA11, RPN1, and SLC7A11 were increased, while GYS1 expression was decreased (Fig. 2b).Afterwards, the correlation analysis was employed to identify associations among these four genes (Fig. 2c-d).

Immune Infiltration in COPD

An examination was conducted to compare the immune cell composition of the control and COPD groups. Quantification of differences in 22 infiltrating immune cell types between the control and COPD groups was performed using the CIBERSORT algorithm (Fig. 3a-b). In the COPD group, there was a notable rise in the number of follicular helper T cells and M0-macrophages, while the count of CD8 T cells, activated NK cells, and M2-macrophages showed a significant decline.Furthermore, the presence of neutrophils, activated NK cells, Plasma cells, and resting CD4 memory T cells showed an association with DRGs (Fig. 3c). Given that data was from lung tissue microarray, it will be critical to generate abundance score as oppose to relative abundance. The abundance scores of immune cell were exhibited in Fig. 3d. The trend of the score of follicular helper T cells is consistent with the trend of their relative abundance.

DRGs-Clusters in COPD

The 23 COPD samples were grouped using a consensus clustering algorithm based on the expression profiles

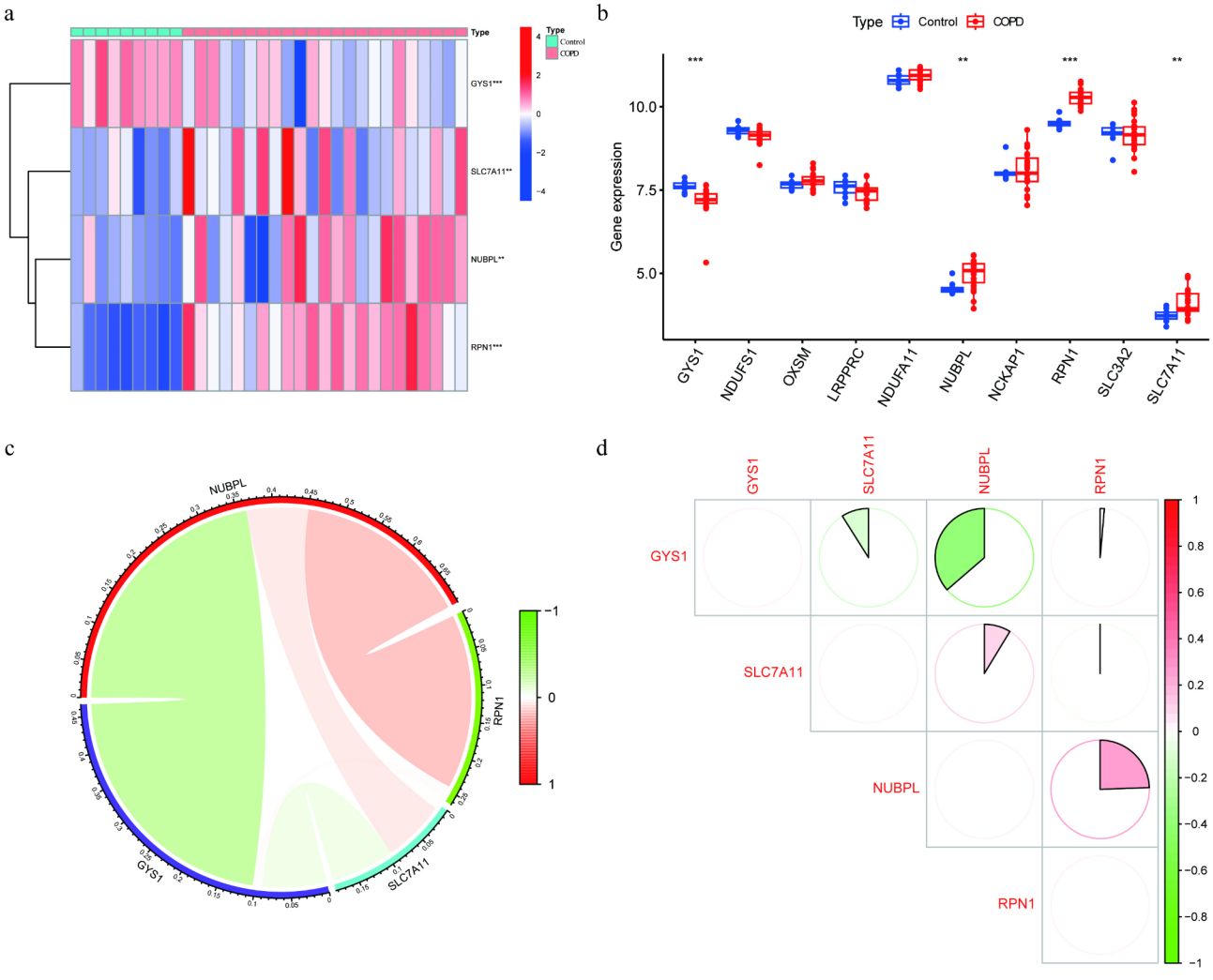

Fig. 2 Identification of DE-DRGs in COPD. **(a)** The expression levels of 4 DE-DRGs were presented in the heatmap.**(b)** The expression levels of DRGs were exhibited between control and COPD groups in boxplots. **(c-d)** Correlation analysis of 4 DE-DRGs. Red and green colors represent positive and negative correlations, respectively. *$p<0.05$, **$p<0.01$, ***$p<0.001$

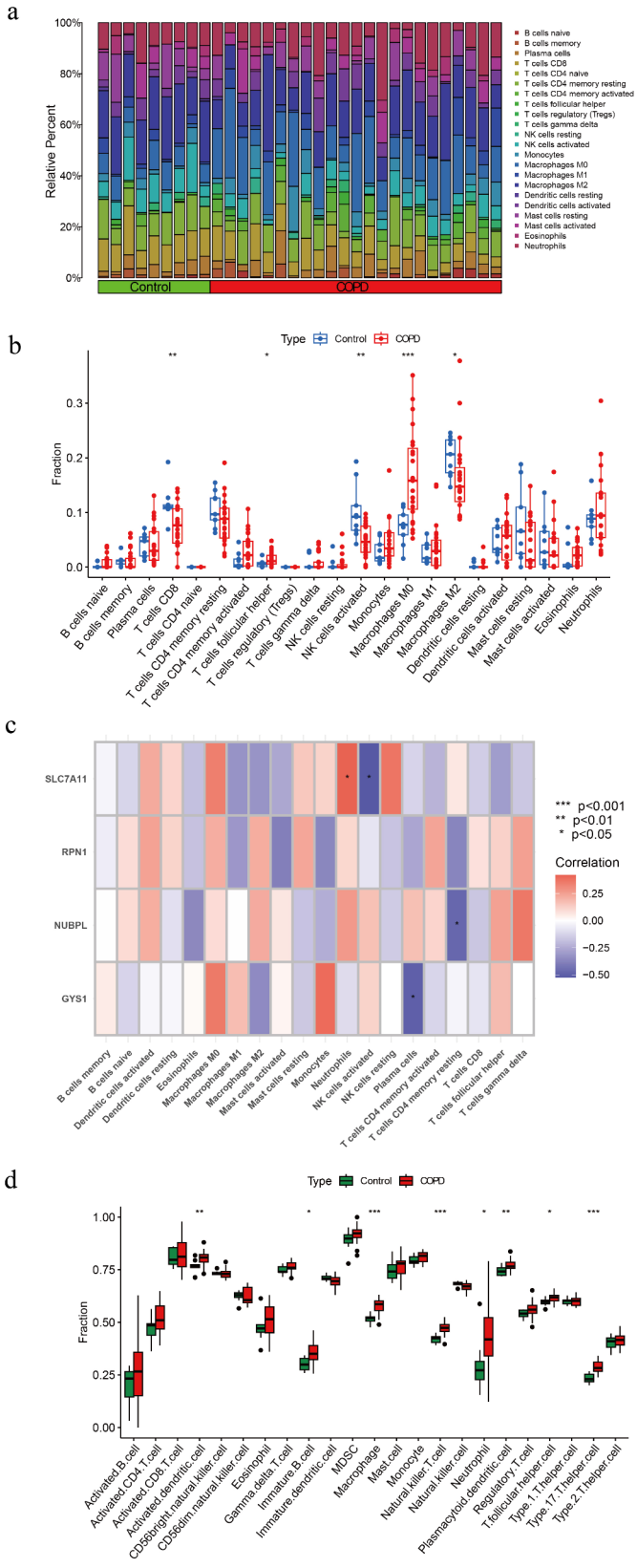

Fig. 3 immune infiltration in COPD.**(a)** The difference in abundance of 22 infiltrating immune cell types between control and COPD groups. **(b)** The differences in immune infiltration between control and COPD groups are shown in the boxplot. **(c)** correlation analysis between four DE-DRGs and infiltrated immune cells. **(d)** The scores of immune cell between control and COPD groups are shown

of the 4 DE-DRGs. The optimal cluster number was achieved when the value of k was set to 2 (Fig. 4a-b). On the other hand, for values of k ranging from 2 to 9, there was a disparity in the area beneath the two cumulative distribution function curves (k and K-1) (Fig. 4c). he highest consistency score of each subtype was observed when k = 2 (Fig. 4d).According to PCA, the 23 patients diagnosed with COPD were divided into two groups called Cluster 1 ($n = 11$) and Cluster 2 ($n = 12$), and notable distinctions were observed between these two clusters (Fig. 4e).

Differences in DRGs and immune infiltration levels between the DRGs-Clusters

Comprehensive evaluation was conducted to examine the molecular traits of both clusters and analyze their disparities in DRGs. The presentation of DRGs in Cluster 1 and Cluster 2 was illustrated(Fig. 5a). Notably, the NUBPL expression level exhibited a decline in Cluster 2 (Fig. 5b).Furthermore, examination of levels of immune cell infiltration indicated variations in the immune microenvironment of Cluster 1 and Cluster 2 (Fig. 5c). The ratio of resting memory CD4 T cells was considerably greater in Cluster 2 (Fig. 5d). The abundance score of immune cell between the two Clusters were exhibited in Fig. 5e. However, no significant difference was observed in the abundance score of immune cell between the two Clusters (Fig. 5e).

Biological functions and pathway activities based on GSVA

GSVA was used to identify pathway activities and biological functions.Cluster 1 showed enrichment of regulatory processes for exiting mitosis, phosphotransferase activity involving phosphate group as the acceptor, MCM complex, and mismatch repair.In contrast, Cluster 2 exhibited enrichment in the regulation of ion transport, hematopoiesis regulation, positive regulation of cell differentiation, and maintenance of divalent inorganic cation homeostasis (Fig. 6a). The KEGG pathway analysis showed that omplement and coagulation cascades, nodlike receptor signaling pathway, type II diabetes mellitus, and Fc γ-mediated phagocytosis were increased in Cluster 1. Additionally, Cluster 2 exhibited enrichment in lysine degradation, base excision repair, DNA replication, Parkinson's disease, and Huntington disease (Fig. 6b).

Gene module screening and co-expression network construction

To construct the distinct color co-expression modules and the heat map of the topological overlap matrix

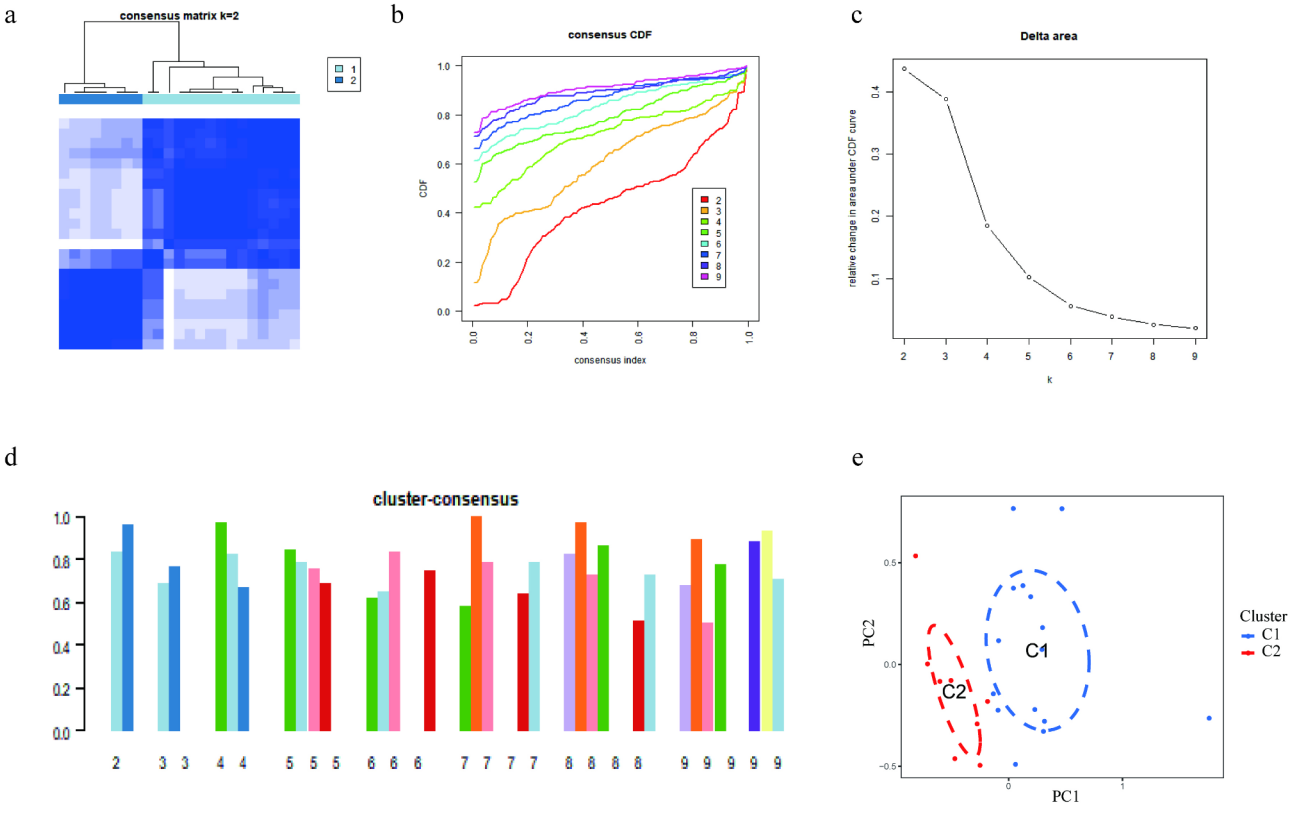

Fig. 4 Identification of cuproptosis-related molecular clusters in COPD. **(a)** The cluster number was most stable when the k value was set to 2. **(b)** the CDF curve fluctuates within the minimum range of the consensus index of 0.2 to 0.6. **(c)** the area under the CDF curve shows the difference between the two CDF curves. **(d)** when k = 2, the concordance score of each subtype was the highest. **(e)** PCA showed significant differences between the two clusters

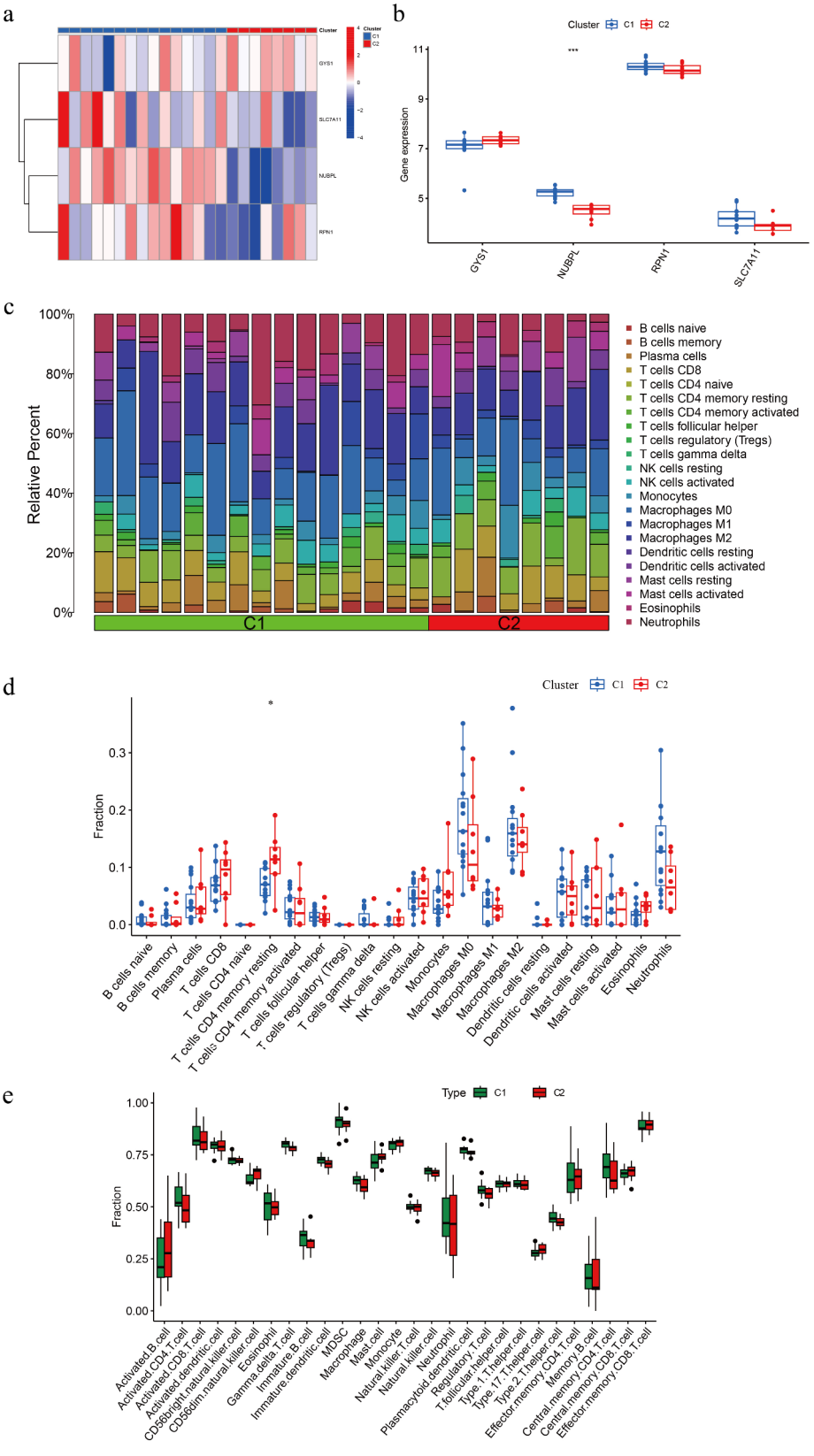

Fig. 5 Differentiation of DRGs and immune infiltration between the DRGs-Clusters. **(a)** Different DRGs expression landscapes were exhibited in the heatmap. **(b)** the expression of DRGs between two clusters was presented in the boxplot. **(c)** The difference in the abundance of 22 infiltrating immune cell types between the two clusters. **(d)** The differences in immune infiltration between the two clusters are shown in a boxplot. **(e)** The abundance score of immune cell between the two Clusters are shown in a boxplot

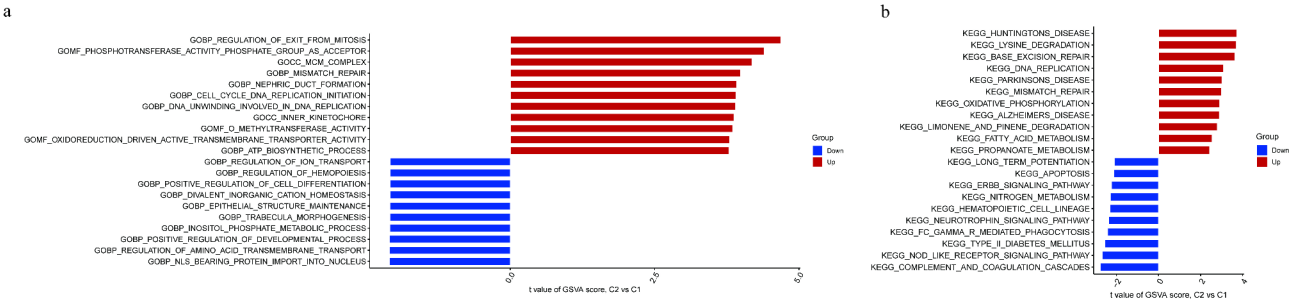

Fig. 6 Biological functions and pathway activities between two CRG clusters. **(a)** Differences in biological functions between Clusters 1 and 2 samples ranked by t-value of GSVA method. **(b)** Differences in hallmark pathway activities between Clusters 1 and 2 samples ranked by the t-value of the GSVA method

(TOM), the dynamic cutting algorithm was employed. Out of these, a total of 759 genes in the blue module were found to be linked with COPD (Fig. 7a). Moreover, the WGCNA algorithm was employed to examine the crucial gene modules that are strongly associated with DRG clusters.The analysis of the relationship between modular clinical features (Cluster 1 and Cluster 2) revealed that 591 genes in the blue module exhibited a strong correlation with COPD clusters (Fig. 7b). Two modules were analyzed using the 'Venn' R package, resulting in the identification of 9 intersection genes. (Fig. 7c).

Construction of machine learning models

Four machine-learning models, namely RF, SVM, GLM, and XGB, were established using cluster-specific DEGs in the training cohort of COPD. We used the "DALEX" R package to interpret the four models and plot the residual distribution. GLM machine learning models demonstrated a comparatively low residual value (Fig. 8a-b). Subsequently, the genes for the top 15 important features of each model were verified based on root-mean-square error (RMSE) (Fig. 8c). Furthermore, the discriminatory efficacy of the four machine learning models was assessed by generating receiver operating characteristic (ROC) curves using 5-fold cross-validation in the training set (GSE38974 dataset) (Fig. 8d). In addition, the AUC values in the four models were exhibited (RF, AUC = 0.833; SVM, AUC = 0.917; XGB, AUC = 0.792; GLM, AUC = 0.667). The SVM machine learning model performed better than the other models in differentiating COPD patients with various clusters, based on the residual value and AUC. Finally, the top five most important genes (MMP9, TMEM27, ZNF785, ZNRF3, and IPPK) from the GLM model were selected as predictor genes for the ensuing analyses.

Construction of nomogram model

A nomogram was constructed to estimate the risk of cuproptosis clusters in 23 COPD patients (Fig. 9a). Next, correction curve and decision curve analysis (DCA) were employed to test its predictive efficiency. According to the calibration curve, the error between the actual risk and the predicted risk of the COPD cluster was small (Fig. 9b). At the same time, DCA indicated that the nomogram had high accuracy and could assist in clinical decision-making (Fig. 9c).

Assessment of machine learning models

The GSE76925 dataset was employed to verify the accuracy of the machine-learning model. In the GSE76925 dataset, the AUC value of the ROC curve of the SVM model, which incorporated five genes (MMP9, TMEM27, ZNF785, ZNRF3, and IPPK), was determined to be 0.907 (Fig. 10a). The correlations between clinical traits of COPD patients were subsequently examined in the GSE76925 dataset (Fig. 10b-l). Briefly, ZNF785 was positively correlated with age ($R = 0.27$), IPPK was negatively correlated with age ($R = -0.34$) and FEV1.pp ($R = -0.32$) and positively correlated with pi10 ($R = 0.35$), ZNRF3 was negatively correlated with BMI ($R = -0.25$) and perc15 ($R = -0.23$) and positively correlated with laa950 ($R = 0.23$), TMEM27 was negatively correlated with BMI ($R = -0.20$) and FEV1.pp ($R = -0.20$), ZANF785 was positively correlated with FEV1.pp ($R = 0.21$), and lastly, iPPK was negatively correlated with FEV1/FVC ($R = -0.26$).

Discussion

Disulfidptosis and COPD

Previous studies demonstrated that the content of disulfide is increased in the sputum of COPD patients, which may be involved in disulfidptosis [25, 26, 31]. Based on this evidence, we hypothesized that disulfidptosis may play a decisive role in the pathogenesis of COPD. To the best of our knowledge, this is the first study to comprehensively analyze the expression profile of DRGs in healthy subjects and COPD patients. More importantly, the results exposed significant differences in the expression level of NDUFA11, RPN1, SLC7A11, and GYS1 in COPD patients compared with the healthy population. NDUFA11 is a crucial respiratory chain protein in mitochondria, and its abnormal expression or structure may lead to defects in the cellular respiratory chain [38].

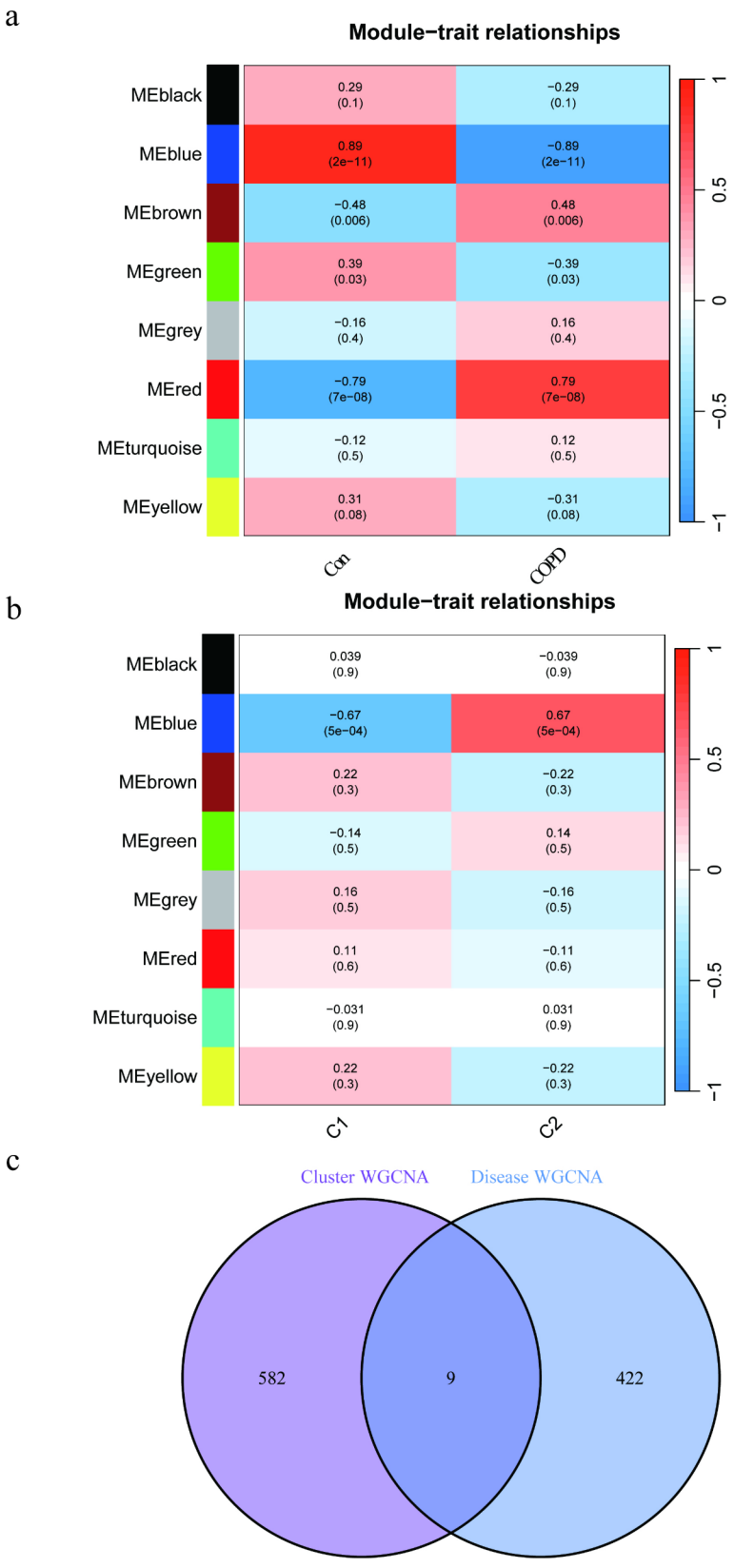

Fig. 7 Gene modules and coexpression network. **(a)** Correlation analysis between module eigengenes and clinical status in control and COPD groups. **(b)** Correlation analysis between module eigengenes and clinical status in the two clusters. Each row represents a module; each column represents a clinical status. **(c)** Identification of the intersected genes of disease WGCNA and cluster-WGCNA

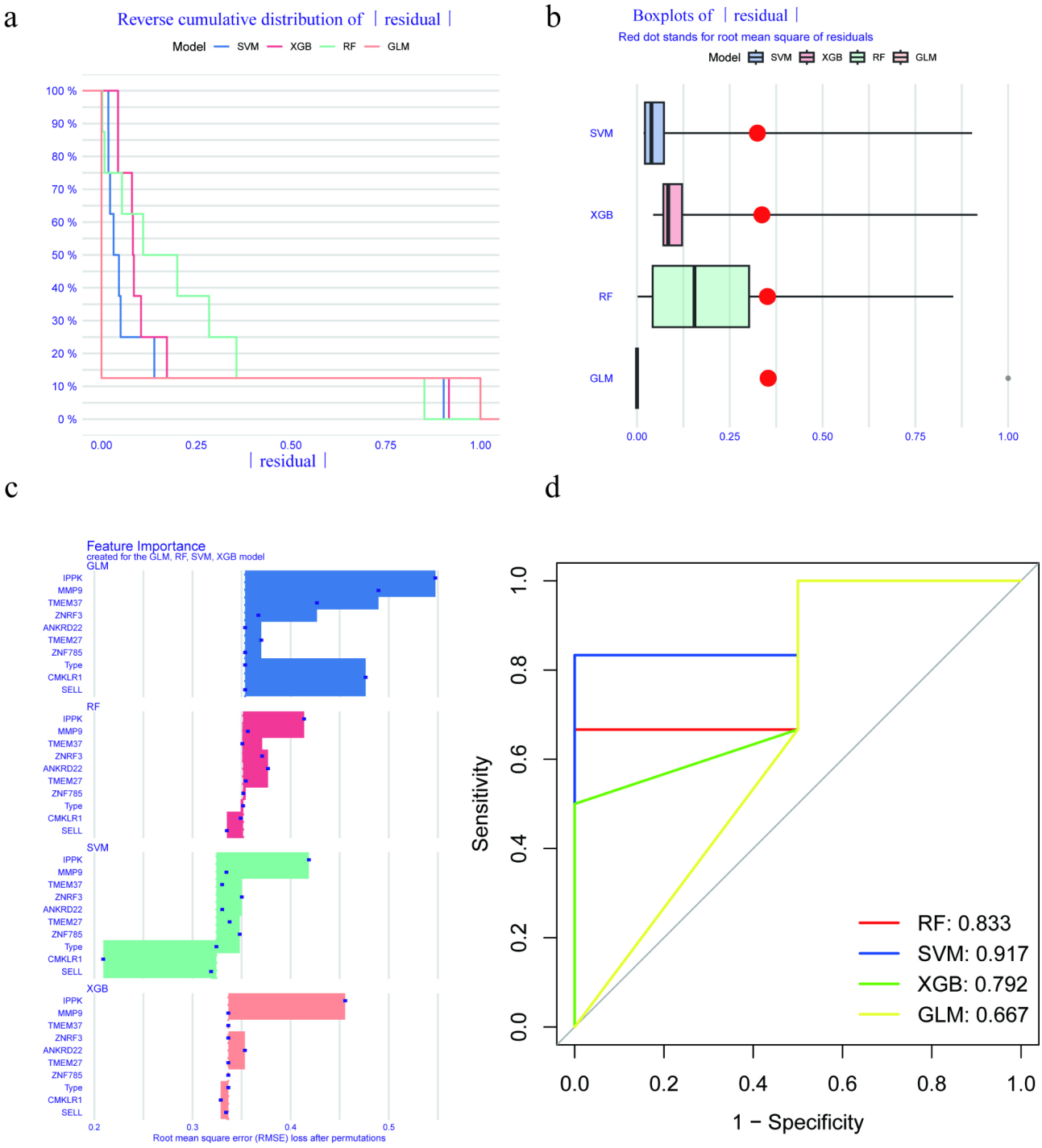

Fig. 8 Construction of machine learning models. **(a)** Residual distribution of each machine learning model. **(b)** The residuals of each machine-learning model are shown in boxplots. **(c)** The important features in machine learning models. **(d)** ROC analysis of four machine learning models based on 5-fold cross-validation in the testing cohort

In the current study, the expression of NDUFA11 was up-regulated in COPD individuals, insinuating that the cell respiratory chain may be damaged. The ability of cells to resist disulfidptosis can be enhanced by knocking down RPN1, which encodes an N-oligosaccharyl transferase located in the endoplasmic reticulum [39]. In this study, the expression level of RPN1 was elevated in COPD patients, inferring that COPD patients are more prone to disulfidptosis. SLC7A11, also referred to as solute carrier family 7 member 11, forms a protein complex

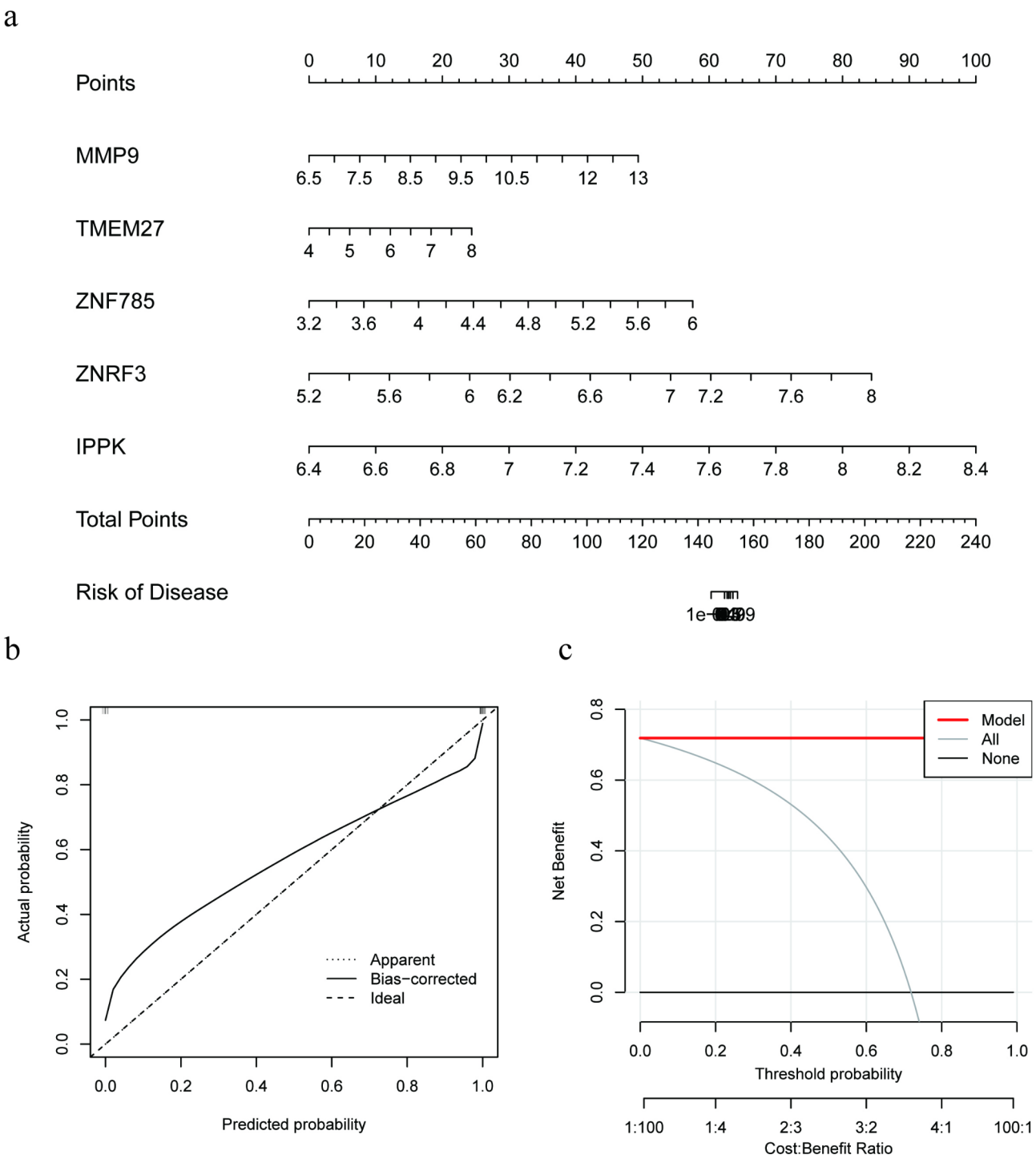

Fig. 9 Validation of the 5-gene-based SVM model. **(a)** Construction of a nomogram for predicting the risk of COPD clusters based on the 5-gene-based SVM model. **(b-c)** Construction of calibration curve

with SLC3A2 that stimulates cystine to migrate intracellularly and accumulate; it can also stimulate the generation of abnormal disulfide bonds in the cytoskeleton protein actin and F-actin collapse, ultimately leading to cell death [29, 39, 40]. The up-regulated expression of SLC7A11 in COPD patients also signifies an increase in the abundance of the SLC7A11-SLC3A2 complex, which contributes to disulfidptosis. GYS1 (also known as glycogen synthase 1) plays an instrumental role in governing glycogen metabolism and enhancing glycogen synthesis [41]. A reduction of GYS1 in COPD patients limits glycogen synthesis, decreases intracellular glycogen storage,

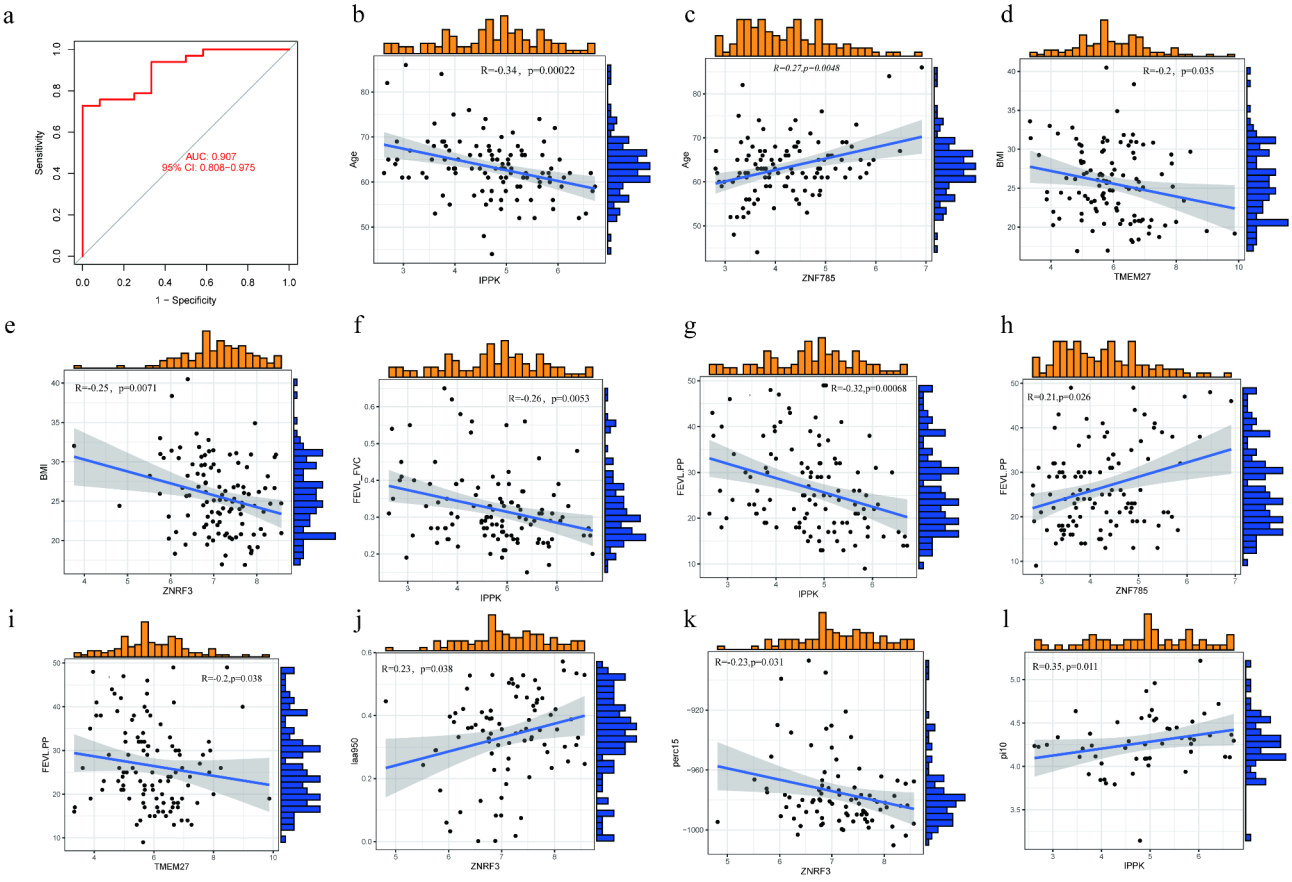

Fig. 10 Validation of correlation analysis based on GSE76925 dataset. **(a)** the ROC curve of the five genes of SVM model. **(b)** Correlation between the IPPK and age. **(c)** Correlation between the ZNF785 and age. **(d)** Correlation between the TMEM27 and BMI. **(e)** Correlation between the ZNRF3 and BMI. **(f)** Correlation between the IPPK and FEV1/EVC. **(g)** Correlation between the IPPK and FEV1/FVC. **(h)** Correlation between the IPPK and FEV1PP. **(i)** Correlation between the ZNF785 and FEV1PP. **(j)** Correlation between the ZNRF3 and laa950. **(k)** Correlation between the ZNRF3 and perc15. **(l)** Correlation between the IPPK and pi10

and further facilitates bacterial proliferation in the lung, thereby aggravating COPD [42].

The relation between immune cells and COPD

The airway and lung tissues of COPD patients trigger a sustained innate and adaptive immune inflammatory response involving neutrophils, macrophages, T lymphocytes, and other immune cells [43, 44]. Jogdand et al. identified differences in eosinophil count in the lung tissue of COPD patients and claimed that these cells may play a regulatory role in bronchioles, alveolar parenchyma, and ectopic lymphocyte aggregation [45].

Although the LM22 signature matrix was utilized to evaluate immune cells in lung tissue [46–48], gene sets from blood-based immune cells may not be transferred well enough to analyze the lung transcriptome. Therefore, in addition to the LM22 signature matrix, we also used ssGSEA to analyze immune cells in lung tissue. Based on LM22 signature matrix and ssGSEA, we found the follicular helper T cells (fhT) may play the crucial role in COPD. fhT plays a key intermediate role in the antibody response between dendritic cells (DC), T cells, and B cells [49]. In other words, fhT first interacts with DC before migrating to follicular B cells [50]. Nevertheless, its differentiation is strictly controlled. Besides, fhT may be regulated by cytotoxic T lymphocyte antigen 4 (CTLA4). Shen et al. theorized that CTLA 4 levels were related to lung function and inflammation in chronic obstructive pulmonary disease [51]. An increase in the number of fhT can impact the proportion of B cells, which is conducive to the occurrence and development of COPD or even lead to exacerbation [52, 53].

DRGs-Clusters in COPD

In molecular biology, we are often interested in determining the group structure in cell populations or microarray gene expression data [54]. Based on the microarray gene expression data, observation subjects could be identified in similar observation groups [55]. In this study, DE-DRGs were utilized to cluster and divide COPD patients into two observation groups, namely Cluster 1 and Cluster 2. The mutation in NUBL (named Nucleotide

Binding Protein-Like) was considered to be associated with nervous system diseases [56, 57]. The abnormality in NUBL can potentially trigger mitochondrial damage [58], indicating that pulmonary cells of Cluster 1 patients exhibited mitochondrial function impairment.

Muthu K Shanmugam et al. described that epigenetic inheritance may be involved in COPD [59]. In the present study, the regulation of exit from mitosis, mismatch repair, and MCM complex was significantly increased in Cluster 1 patients. Abnormal functioning of the DNA mismatch repair system can trigger COPD and may be related to alterations in microsatellite (MS) DNA [60]. Therefore, attention should be paid to fluctuations in epigenetics in Cluster 1 patients. In addition, the KEGG result of KEGG pathway analysis exposed that Fc γ-mediated phagocytosis was enriched in Cluster 1. FcγR (Fc γ receptors) are receptors on the C-terminal of the Fc portion of IgG that mediate the antigen-antibody complex on cells and play a key role in the pathogenesis of COPD [61]. Fc γ-mediated phagocytosis may be considered as a new therapeutic target for these patients in Cluster (1) In contrast, regulation of ion transport and regulation of hematopoiesis were enriched in Cluster (2) Abnormal fluctuations in ion transport, such as abnormal transfer of sodium and chloride ions, can lead to increased mucus secretion, which exacerbates respiratory obstruction in COPD patients [62]. Stefan Kuhnert highlighted that clonal hematopoiesis of indeterminate potential may be related to inflammatory gene expression in COPD patients [63]. Interestingly, Parkinson's disease(PD) was enriched in Cluster 2. The potential link between COPD and PD remains unclear. Previous study suggested that Elevated PM2.5 concentrations may increase the risk of PD in the individual with COPD [64].

Machine learning model and COPD

To date, no treatment has been shown to halt or reverse the progression of COPD, and consequently, there is an urgent need for a timely diagnosis. Multiple studies have recently sought to identify undiagnosed COPD and establish approaches for its early diagnosis, and their value will ultimately be determined by the impact of interventions on the disease [65]. To better diagnose diseases, disease prediction models based on special molecular markers have been used [66].

Based on the expression profiles of cluster-specific DRGs, the predictive performance of the four selected machine learning models (RF, SVM, GLM, XGB) for COPD was compared, and the results uncovered that the GLM model was more accurate in predicting COPD. Based on the GLM model, the five most important genes (MMP9, TMEM27, ZNF785, ZNRF3, and IPPK) were selected as predictor genes and used to construct the predictive model. Nevertheless, The AUC curve is obtained with a tiny number of samples therefore, it is challenging to compare AUCs, for example the standard error would be huge. Therefore, the external data as testing set was used for validation. Another dataset of COPD was thereupon utilized to test the accuracy of the model, and the results showed that the AUC of the predictive model was 0.907, signifying satisfactory accuracy. Moreover, these five predictor genes were used to correlate clinical traits in patients with COPD. Four genes, including ZNF785, IPPK, ZNRF3, and TMEM27, were found to be significantly correlated with age, BMI, FEV1PP, FEV1/FVC, laa950, and perc15.

Old age and high BMI are risk factors for COPD [67, 68]. FEV1PP and FEV1/FVC, indicators of lung function, are critical parameters for the diagnosis of COPD [69, 70]. The perc15 is defined as the density value in HU below which 15% of the lung voxels are found [71]. The higher the pec15 value, the more active the lung inflammation [71]. Laa950 is a common threshold used to diagnose emphysema and is positively correlated with the severity of COPD [72]. Pi10 is considered an imaging biomarker of disease severity, decreased lung function, and mortality in individuals with COPD [73]. Meanwhile, IPPK (as known as inositol 1,3,4,5, 6-Pentakisphosphate 2-kinase) was negatively correlated with age, FEV1PP, and FEV1/FVC and positively correlated with pi10. In this study, IPPK was positively correlated with Pi10 and negatively correlated with FEV1PP and FEV1/FVC, indicating that it may aggravate lung tissue inflammation and inhibit respiratory function. ZNRF3 (Zinc and ring finger 3) can suppress the Wnt signaling pathway [74], which plays a key role in inhibiting goblet cell metaplasia and mucus secretion, thus alleviating the symptoms of COPD [75]. ZNF785 (zinc finger protein 785) was positively correlated with age and FEV1.PP, but its biological function remains unknown. TMEM27 (Transmembrane protein 27) was found to be expressed in β cells of the pancreatic islet and is related to the pathogenesis of diabetes [76], but its role in the respiratory system deserves further investigation. Therefore, the machine learning model base on disulfidptosis may serve as an early indicator and reliable predictor of systemic dysfunction, making it crucial for predicting and preventing COPD.

There are still some limitations to our research that cannot be overlooked. First of all, the research was based on a comprehensive bioinformatics analysis, and further clinical or experimental evaluation is necessary to verify the expression levels of DRGs. Secondly, bulk and scRNA-seq should be performed in our future work. Lastly, additional COPD samples are required to identify disulfidptosis-related clusters and the machine learning models.

Conclusion

In summary, our study revealed an association between DRGs and COPD. Based on the 5 predicted genes, the GLM model was regarded as the optimal machine learning model and could accurately evaluate the clinical symptoms of COPD patients. Our study is the first to identify the role of disulfidptosis in COPD and further elucidate the underlying molecular mechanisms that contribute to COPD heterogeneity.

Supplementary Information

The online version contains supplementary material available at https://doi.org/10.1186/s12920-024-02076-2.

Supplementary Material 1

Acknowledgements
We thank Home for Researchers editorial team (www.home-for-researchers.com) for language editing service.

Author contributions
Sijun Li and Qingdong Zhu contributed equally to this work. Sijun Li and Qingdong Zhu equally to the study's inception and design. Aichun Huang, Yanqun Lan, Xiaoying Wei, Huawei He, Xiayan Meng and Weiwen Li performed bioinformatics analyses and assisted with the analysis of other data. Yanrong Lin and Shixiong Yang helped to revise the manuscript. All authors have read and approved the fnal manuscript.

Funding
This study was supported by grants from Guangxi Zhuang Autonomous Region Health and Family Planning Commission (Grant No.Z20211324 and No. ZA20231211).

Data availability
The datasets analyzed during the current study are available in the"GSE38974 and GSE76925". (https://www.ncbi.nlm.nih.gov/gds)

Declarations

Ethics approval and consent to participate
Not applicable.

Consent for publication
Not applicable.

Competing interests
The authors declare no competing interests.

Author details
[1]Infectious Disease Laboratory, The Fourth People's Hospital of Nanning, Nanning, China
[2]Department of Tuberculosis, The Fourth People's Hospital of Nanning, Nanning, China
[3]Administrative Office, The Fourth People's Hospital of Nanning, Nanning, China

Received: 6 February 2024 / Accepted: 19 December 2024
Published online: 08 January 2025

References

1. Christenson SA, Smith BM, Bafadhel M, Putcha N. Chronic obstructive pulmonary disease. Lancet. 2022;399(10342):2227–42.
2. Aldonyte R, Bagdonas E, Raudoniute J, Bruzauskaite I. Novel aspects of pathogenesis and regeneration mechanisms in COPD. Int J Chronic Obstr Pulm Dis 2015.
3. Roth GA, Abate D, Abate KH, Abay SM, Abbafati C, Abbasi N, Abbastabar H, Abd-Allah F, Abdela J, Abdelalim A, et al. Global, regional, and national age-sex-specific mortality for 282 causes of death in 195 countries and territories, 1980–2017: a systematic analysis for the global burden of Disease Study 2017. Lancet. 2018;392(10159):1736–88.
4. Zhu B, Wang Y, Ming J, Chen W, Zhang L. Disease burden of COPD in China: a systematic review. Int J Chronic Obstr Pulm Dis. 2018;13:1353–64.
5. Yang IA, Jenkins CR, Salvi SS. Chronic obstructive pulmonary disease in never-smokers: risk factors, pathogenesis, and implications for prevention and treatment. Lancet Respiratory Med. 2022;10(5):497–511.
6. Vij N, Chandramani-Shivalingappa P, Van Westphal C, Hole R, Bodas M. Cigarette smoke-induced autophagy impairment accelerates lung aging, COPD-emphysema exacerbations and pathogenesis. Am J Physiology-Cell Physiol. 2018;314(1):C73–87.
7. Jarad N. Chronic obstructive pulmonary disease (COPD) and old age? Chronic Resp Dis. 2011;8(2):143–51.
8. Ritchie AI, Wedzicha JA. Definition, causes, Pathogenesis, and consequences of Chronic Obstructive Pulmonary Disease exacerbations. Clin Chest Med. 2020;41(3):421–38.
9. Dang-Tan T, Ismaila A, Zhang S, Zarotsky V, Bernauer M. Clinical, humanistic, and economic burden of chronic obstructive pulmonary disease (COPD) in Canada: a systematic review. BMC Res Notes 2015, 8(1).
10. Zhu T, Li S, Wang J, Liu C, Gao L, Zeng Y, Mao R, Cui B, Ji H, Chen Z. Induced sputum metabolomic profiles and oxidative stress are associated with chronic obstructive pulmonary disease (COPD) severity: potential use for predictive, preventive, and personalized medicine. EPMA J. 2020;11(4):645–59.
11. Wise RA, Tashkin DP. Preventing Chronic Obstructive Pulmonary Disease: what is known and what needs to be done to make a difference to the patient? Am J Med. 2007;120(8):S14–22.
12. Petrie K, Toelle BG, Wood-Baker R, Maguire GP, James AL, Hunter M, Johns DP, Marks GB, George J, Abramson MJ. Undiagnosed and misdiagnosed chronic obstructive Pulmonary Disease: data from the BOLD Australia study. Int J Chronic Obstr Pulm Dis. 2021;16:467–75.
13. Bourbeau. AgustíA, Han J. MK: Global Initiative for Chronic Obstructive Lung Disease 2023 Report: GOLD Executive Summary. *The European respiratory journal* 2023, 61(4):2300239.
14. Woodruff PG, Barr. RG BE, Christenson. SA, Couper. D, Curtis. JL: clinical significance of symptoms in smokers with preserved pulmonary function. N Engl J Med. 2016;374(19):1811–21.
15. Qin Q, Gu Z, Li F, Pan Y, Zhang T, Fang Y, Zhang L. A diagnostic model for Alzheimer's Disease based on blood levels of Autophagy-related genes. Front Aging Neurosci 2022, 14.
16. Lai Y, Lin C, Lin X, Wu L, Zhao Y, Lin F. Identification and immunological characterization of cuproptosis-related molecular clusters in Alzheimer's disease. Front Aging Neurosci 2022, 14.
17. Liu K, Cai Y, Song K, Yuan R, Zou J. Clarifying the effect of gut microbiota on allergic conjunctivitis risk is instrumental for predictive, preventive, and personalized medicine: a mendelian randomization analysis. EPMA J. 2023;14(2):235–48.
18. Fabbri LM, Rabe KF. From COPD to chronic systemic inflammatory syndrome? Lancet. 2007;370(9589):197–9.
19. Araya J, Tsubouchi K, Sato N, Ito S, Minagawa S, Hara H, Hosaka Y, Ichikawa A, Saito N, Kadota T, et al. PRKN-regulated mitophagy and cellular senescence during COPD pathogenesis. Autophagy. 2018;15(3):510–26.
20. Mallia-Milanes B, Dufour A, Philp C, Solis N, Klein T, Fischer M, Bolton CE, Shapiro S, Overall CM, Johnson SR. TAILS proteomics reveals dynamic changes in airway proteolysis controlling protease activity and innate immunity during COPD exacerbations. Am J Physiology-Lung Cell Mol Physiol. 2018;315(6):L1003–14.
21. Yoshida M, Minagawa S, Araya J, Sakamoto T, Hara H, Tsubouchi K, Hosaka Y, Ichikawa A, Saito N, Kadota T et al. Involvement of cigarette smoke-induced epithelial cell ferroptosis in COPD pathogenesis. Nat Commun 2019, 10(1).
22. Van Eeckhoutte HP, Donovan C, Kim RY, Conlon TM, Ansari M, Khan H, Jayaraman R, Hansbro NG, Dondelinger Y, Delanghe T et al. RIPK1 kinase-dependent inflammation and cell death contribute to the pathogenesis of COPD. Eur Respir J 2023, 61(4).
23. Wunnapuk K, Pothirat C, Manokeaw S, Phetsuk N, Chaiwong W, Phuackchantuck R, Prapamontol T. PM10-related DNA damage, cytokinetic defects, and

cell death in COPD patients from Chiang Dao district, Chiang Mai, Thailand. Environ Sci Pollut Res. 2019;26(24):25326–40.
24. Lu Z, Van Eeckhoutte HP, Liu G, Nair PM, Jones B, Gillis CM, Nalkurthi BC, Verhamme F, Buyle-Huybrecht T, Vandenabeele P, et al. Necroptosis Signaling promotes inflammation, Airway Remodeling, and Emphysema in Chronic Obstructive Pulmonary Disease. Am J Respir Crit Care Med. 2021;204(6):667–81.
25. Liu X, Nie L, Zhang Y, Yan Y, Wang C, Colic M, Olszewski K, Horbath A, Chen X, Lei G, et al. Actin cytoskeleton vulnerability to disulfide stress mediates disulfidptosis. Nat Cell Biol. 2023;25(3):404–14.
26. Liu X, Olszewski K, Zhang Y, Lim EW, Shi J, Zhang X, Zhang J, Lee H, Koppula P, Lei G, et al. Cystine transporter regulation of pentose phosphate pathway dependency and disulfide stress exposes a targetable metabolic vulnerability in cancer. Nat Cell Biol. 2020;22(4):476–86.
27. Joly JH, Delfarah A, Phung PS, Parrish S, Graham NA. A synthetic lethal drug combination mimics glucose deprivation–induced cancer cell death in the presence of glucose. J Biol Chem. 2020;295(5):1350–65.
28. Koppula P, Zhang Y, Shi J, Li W, Gan B. The glutamate/cystine antiporter SLC7A11/xCT enhances cancer cell dependency on glucose by exporting glutamate. J Biol Chem. 2017;292(34):14240–9.
29. Liu X, Zhang Y, Zhuang L, Olszewski K, Gan B. NADPH debt drives redox bankruptcy: SLC7A11/xCT-mediated cystine uptake as a double-edged sword in cellular redox regulation. Genes Dis. 2021;8(6):731–45.
30. Koppula P, Zhang Y, Zhuang L, Gan B. Amino acid transporter SLC7A11/xCT at the crossroads of regulating redox homeostasis and nutrient dependency of cancer. Cancer Commun. 2018;38(1):1–13.
31. Beeh KM, Koppenhoefer. BJ, Buhl N. Increased glutathione disulfide and nitrosothiols in sputum supernatant of patients with stable COPD. Chest. 2004;126(4):1116–22.
32. Li S, Long Q, Nong L, Zheng Y, Meng X, Zhu Q. Identification of immune infiltration and cuproptosis-related molecular clusters in tuberculosis. Front Immunol. 2023;14:1205741.
33. Ezzie ME, Crawford M, Cho J-H, Orellana R, Zhang S, Gelinas R, Batte K, Yu L, Nuovo G, Galas D, et al. Gene expression networks in COPD: microRNA and mRNA regulation. Thorax. 2012;67(2):122–31.
34. Morrow JD, Zhou X, Lao T, Jiang Z, DeMeo DL, Cho MH, Qiu W, Cloonan S, Pinto-Plata V, Celli B, et al. Functional interactors of three genome-wide association study genes are differentially expressed in severe chronic obstructive pulmonary disease lung tissue. Sci Rep. 2017;7:44232.
35. Hambright WS, Fonseca RS, Chen L, Na R, Ran Q. Ablation of ferroptosis regulator glutathione peroxidase 4 in forebrain neurons promotes cognitive impairment and neurodegeneration. Redox Biol. 2017;12:8–17.
36. Newman AM, Liu CL, Green MR, Gentles AJ, Feng W, Xu Y, Hoang CD, Diehn M, Alizadeh AA. Robust enumeration of cell subsets from tissue expression profiles. Nat Methods. 2015;12(5):453–7.
37. YujuanYou., Chen S, BinquanTang. XX, Deng. H, Wu Y. Exosome-related gene identification and diagnostic model construction in hepatic ischemiareperfusion injury. Sci Rep. 2024;24:22450.
38. Berger I, Hershkovitz E, Shaag A, Edvardson S, Saada A, Elpeleg O. Mitochondrial complex I deficiency caused by a deleterious NDUFA11 mutation. Ann Neurol. 2008;63(3):405–8.
39. Liu X, Nie L, Zhang Y, Yan Y, Wang C, Colic M, Olszewski K, Horbath A, Chen X, Lei G et al. Actin cytoskeleton vulnerability to disulfide stress mediates disulfidptosis. Nat Cell Biol 2023.
40. Koppula P, Zhang Y, Zhuang L, Gan B. Amino acid transporter SLC7A11/xCT at the crossroads of regulating redox homeostasis and nutrient dependency of cancer. Cancer Commun (Lond). 2018;38(1):12.
41. Skurat AV, Dietrich AD, Roach PJ. Interaction between glycogenin and glycogen synthase. Arch Biochem Biophys. 2006;456(1):93–7.
42. Sadiku P, Willson JA, Ryan EM, Sammut D, Coelho P, Watts ER, Grecian R, Young JM, Bewley M, Arienti S, et al. Neutrophils fuel effective Immune responses through Gluconeogenesis and Glycogenesis. Cell Metab. 2021;33(2):411–23. e414.
43. Feghali-Bostwick CA, Gadgil AS, Otterbein LE, Pilewski JM, Stoner MW, Csizmadia E, Zhang Y, Sciurba FC, Duncan SR. Autoantibodies in patients with chronic obstructive pulmonary disease. Am J Respir Crit Care Med. 2008;177(2):156–63.
44. Laucho-Contreras ME, Polverino F, Gupta K, Taylor KL, Kelly E, Pinto-Plata V, Divo M, Ashfaq N, Petersen H, Stripp B, et al. Protective role for club cell secretory protein-16 (CC16) in the development of COPD. Eur Respir J. 2015;45(6):1544–56.
45. Jogdand P, Siddhuraj P, Mori M, Sanden C, Jonsson J, Walls AF, Kearley J, Humbles AA, Kolbeck R, Bjermer L et al. Eosinophils, basophils and type 2 immune microenvironments in COPD-affected lung tissue. Eur Respir J 2020, 55(5).
46. Zheng Y, Tang L, Liu Z. Multi-omics analysis of an immune-based prognostic predictor in non-small cell lung cancer. BMC Cancer 2021, 21(1).
47. Eljilany I, Saghand PG, Chen J, Ratan A, McCarter M, Carpten J, Colman H, Ikeguchi AP, Puzanov I, Arnold S et al. The T cell immunoscore as a reference for Biomarker Development utilizing real-World Data from patients with Advanced malignancies treated with Immune Checkpoint inhibitors. Cancers 2023, 15(20).
48. Jiang Z, Luo Y, Zhang L, Li H, Pan C, Yang H, Cheng T, Chen J. A novel risk score model of Lactate Metabolism for Predicting over Survival and Immune Signature in Lung Adenocarcinoma. Cancers 2022, 14(15).
49. Walker LSK. The link between circulating follicular helper T cells and autoimmunity. Nat Rev Immunol. 2022;22(9):567–75.
50. Victora GD, Nussenzweig MC. Germinal centers. Annu Rev Immunol. 2012;30:429–57.
51. Shen Y, Yang T, Wang T, Chen L, Wen F. Elevated circulating cytotoxic T lymphocyte-associated antigen-4 levels are related to lung function and inflammation in chronic obstructive pulmonary disease. Respirology. 2013;18(5):885–6.
52. van der Strate BW, Postma DS, Brandsma CA, Melgert BN, Luinge MA, Geerlings M, Hylkema MN, van den Berg A, Timens W, Kerstjens HA. Cigarette smoke-induced emphysema: a role for the B cell? Am J Respir Crit Care Med. 2006;173(7):751–8.
53. Hogg JC. Pathophysiology of airflow limitation in chronic obstructive pulmonary disease. Lancet. 2004;364(9435):709–21.
54. Nugent. R, Meila M. An overview of clustering applied to molecular biology. Methods Mol Biol. 2010;620:369–404.
55. Grunig G, Durmus N, Zhang Y, Lu Y, Pehlivan S, Wang Y, Doo K, Cotrina-Vidal ML, Goldring R, Berger KI et al. Molecular clustering analysis of blood biomarkers in World Trade Center exposed community members with persistent lower respiratory symptoms. Int J Environ Res Public Health 2022, 19(13).
56. Chakrabarti VS, Mikolajczyk M, Boscaro F, Calderone V. Human Ind1 expression causes over-expression of E. Coli beta-lactamase ampicillin resistance protein. Protein Expr Purif. 2014;104:26–33.
57. Eis PS, Huang N, Langston JW, Hatchwell E, Schule B. Loss-of-function NUBPL mutation May Link Parkinson's disease to recessive complex I Deficiency. Front Neurol. 2020;11:555961.
58. Dubaisi. KV, RA, Maclean. AE, Hall. K, Weiss. L, Stover. AE, Schwartz. PH, Berg. B, Cheng. C, Parikh et al. S: NUBPL mitochondrial disease: new patients and review of the genetic and clinical spectrum. *J Med Genet* 2021 58(5):314–325.
59. Shanmugam MK, Sethi G. Role of epigenetics in inflammation-associated diseases. Subcell Biochem. 2013;61:627–57.
60. Samara K, Zervou M, Siafakas NM, Tzortzaki EG. Microsatellite DNA instability in benign lung diseases. Respir Med. 2006;100(2):202–11.
61. Titova E, Aune MW, Fonn K, Henriksen AH, Asberg A. Neutrophil CD64 expression as a diagnostic marker in patients hospitalized with exacerbations of COPD: a prospective observational study. Lung. 2015;193(5):717–24.
62. Hill. DB, Button. B, Rubinstein. M, Boucher RC. Physiology and pathophysiology of human airway mucus. Physiol Rev. 2022;102(4):1757–836.
63. Kuhnert S, Mansouri S, Rieger MA, Savai R, Avci E, Diaz-Pina G, Padmasekar M, Looso M, Hadzic S, Acker T et al. Association of Clonal Hematopoiesis of Indeterminate Potential with Inflammatory Gene Expression in Patients with COPD. *Cells* 2022, 11(13).
64. Kuan LC-W, Chen Y-H, W-Y, Chen. C-J, Lin FC-F, Tsai SC-S. Association between PM2.5 exposure and risk of Parkinson's disease in individuals with chronic obstructive pulmonary disease in Taiwan: a nested case-control study. Epidemiol Health. 2023;45:e2023094.
65. Ray E, Culliford D, Kruk H, Gillett K, North M, Astles CM, Hicks A, Johnson M, Lin SX, Orlando R, et al. Specialist respiratory outreach: a case-finding initiative for identifying undiagnosed COPD in primary care. NPJ Prim Care Respir Med. 2021;31(1):7.
66. Li S, Long Q, Nong L, Zheng Y, Meng X, Zhu Q. Identification of immune infiltration and cuproptosis-related molecular clusters in tuberculosis. Front Immunol 2023, 14.
67. Lewthwaite H, Li PZ, O'Donnell DE, Jensen D. Multidimensional breathlessness response to exercise: impact of COPD and healthy ageing. Respir Physiol Neurobiol. 2021;287:103619.
68. McNicholas WT, Hansson D, Schiza S, Grote L. Sleep in chronic respiratory disease: COPD and hypoventilation disorders. Eur Respir Rev 2019, 28(153).

69. Mohamed Hoesein FA, Zanen P, Lammers JW. Lower limit of normal or FEV1/FVC < 0.70 in diagnosing COPD: an evidence-based review. Respir Med. 2011;105(6):907–15.
70. Sheikh S, Putt ME, Forde KA, Rubenstein RC, Kelly A. Elevation of one hour plasma glucose during oral glucose tolerance testing. Pediatr Pulmonol. 2015;50(10):963–9.
71. Jobst BJ, Weinheimer O, Trauth M, Becker N, Motsch E, Gross ML, Tremper J, Delorme S, Eigentopf A, Eichinger M, et al. Effect of smoking cessation on quantitative computed tomography in smokers at risk in a lung cancer screening population. Eur Radiol. 2018;28(2):807–15.
72. Gu S, Li R, Leader JK, Zheng B, Bon J, Gur D, Sciurba F, Jin C, Pu J. Obesity and extent of emphysema depicted at CT. Clin Radiol. 2015;70(5):e14–19.
73. Moslemi A, Kontogianni K, Brock J, Wood S, Herth F, Kirby M. Differentiating COPD and asthma using quantitative CT imaging and machine learning. Eur Respir J 2022, 60(3).
74. Liang JJ, Li HR, Chen Y, Zhou Z, Shi YQ, Zhang LL, Xin L, Zhao DB. ZNRF3 regulates Collagen-Induced Arthritis through NF-kB and wnt pathways. Inflammation. 2020;43(3):1077–87.
75. Kim HT, Yin W, Nakamichi Y, Panza P, Grohmann B, Buettner C, Guenther S, Ruppert C, Kobayashi Y, Guenther A, et al. WNT/RYK signaling restricts goblet cell differentiation during lung development and repair. Proc Natl Acad Sci U S A. 2019;116(51):25697–706.
76. Pepaj M, Gjerlaugsen N, Julien K, Thorsby PM. Tmem27 is upregulated by vitamin D in INS-1 cells and its serumconcentrations are low in patients with autoimmune diabetes. Scand J Clin Lab Invest. 2014 74(4):358–365.

Publisher's note